JOURNAL OF SOLID STATE CHEMISTRY **140,** 29–37 (1998)
ARTICLE NO. SC987818

# Behavior of Ag Admixtures in $Sb_2Te_3$ and $Bi_2Te_3$ Single Crystals

J. Navrátil,*,[1] I. Klichová,† S. Karamazov,† J. Šrámková,† and J. Horák‡

*Joint Laboratory of Solid State Chemistry of the Czech Academy of Sciences and University of Pardubice, Studentská 84, 530 09 Pardubice, Czech Republic; †Faculty of Chemical Technology, University of Pardubice, Čs. Legií 565, 532 10 Pardubice, Czech Republic; and ‡Institute of Inorganic Chemistry of the Czech Academy of Sciences, Pelleova 24, 160 00 Prague, Czech Republic

Received July 22, 1997; in revised form March 12, 1998; accepted March 16, 1998

**Single crystals of $Sb_2Te_3$ doped with Ag ($c_{Ag} = (0–9) \times 10^{19}$ cm$^{-3}$) were prepared from the melt $Sb_{2-x}Ag_xTe_3$ (denoted by a) or the melt $Sb_2Ag_xTe_3$ (denoted by b). The reflectivity in the IR region, electrical conductivity, and Hall coefficient were determined for these crystals. From the reflection spectra values of the high-frequency dielectric constant, optical relaxation time, and plasma resonance frequency were obtained for crystals with various Ag contents. The dependencies of the real ($\varepsilon_1$) and imaginary ($\varepsilon_2$) parts of the dielectric function and the imaginary part of the energy loss function ($\mathrm{Im}(-1/\varepsilon)$) on the wavenumber were also determined. From the $\varepsilon_2(\nu)$ dependence at room temperature, it was concluded that in $Sb_2Te_3$(Ag) crystals the scattering mechanism of free carriers on the acoustical phonons prevails, but the participation of scattering on ionized impurities is also probable. The a- and b-type crystals of $Sb_2Te_3$(Ag) manifested practically the same values of transport coefficients and optical properties in the IR region. The determined values of the Hall coefficient showed that Ag atoms doping the $Sb_2Te_3$ crystal structure behave as acceptors. The incorporation of 1 Ag atom into the crystals prepared from $Sb_{2-x}Ag_xTe_3$ and $Sb_2Ag_xTe_3$ melts increases the hole concentration by about 1.7 holes. This result is interpreted as the incorporation of Ag atoms into the crystal structure in the form of substitutional defects of $Ag''_{Sb}$ with two negative charges. Part of the Ag atoms can form defects of the type $[Ag''_{Sb} + h^{\bullet}]$, i.e., $Ag'_{Sb}$, or be incorporated in the four-layer lamellae $[Te–Ag_{0.5}Sb_{0.5}–Te–Sb_{0.5}Ag_{0.5}]$ as uncharged defects. The Ag atoms incorporated into the $Bi_2Te_3$ structure always behave as donors. The formation of $Ag_i^{\bullet}$ interstitials is proposed as well. The different behavior of Ag atoms in $Sb_2Te_3$ and $Bi_2Te_3$ crystals is probably associated with different parameters of the chemical bonds in these crystals, which is supported by the results of a semiempirical calculation.** © 1998 Academic Press

## 1. INTRODUCTION

The crystals of $Sb_2Te_3$ and $Bi_2Te_3$ belong among the layered semiconducting compounds with the tetradymite structure (space group $R3m$-$D^5_{3d}$); the crystals possess narrow energy gaps of $E_g(Sb_2Te_3) = 0.21$ eV and $E_g(Bi_2Te_3) = 0.13$ eV (1). These compounds doped with various dopants are applied also for the construction of thermoelectric devices such as cooling elements and thermogenerators (2). The trigonal lattice of the tetradymite structure of $Me_2Te_3$ ($Me$ = Sb, Bi) consists of layers, each layer comprising five atomic planes oriented perpendicular to the trigonal axis $c$ and alternating as

$$\ldots\ldots\ \mathrm{Te}^1 Me \mathrm{Te}^2 Me \mathrm{Te}^1\ \ldots\ldots\ \mathrm{Te}^1 Me \mathrm{Te}^2 Me \mathrm{Te}^1\ \ldots\ldots\ ,$$

leaving a van der Waals gap between two neighboring $Te^1$ layers.

The physical properties characterizing these compounds as semiconductors were studied in several papers dealing with their band structure (3–7) and scattering mechanism of free current carriers (8, 9). Thermoelectric properties and transport coefficients of these compounds doped with various foreign atoms were studied as well. Special attention has been devoted to the preparation of materials with a high value of the figure of merit (2).

Despite the considerable attention paid to tetradymite crystals, a detailed study of the effects associated with the incorporation of silver atoms into the structure of $Sb_2Te_3$ and $Bi_2Te_3$ has not been done. Available data in the literature show that the incorporation of Ag atoms into $Sb_2Te_3$ (10) results in an increase in the concentration (11) of holes, whereas the incorporation of Ag into $Bi_2Te_3$ results in a decrease in the hole concentration. The literature data (12–15) describe also the formation, structure, and properties of ternary $AgSbTe_2$ and $AgBiTe_2$ crystals.

In this paper we report the optical properties, electrical conductivity, and Hall coefficient of single-crystalline samples of $Sb_2Te_3$ with various contents of incorporated Ag atoms. Additionally, we compare some physical parameters of Ag-doped $Sb_2Te_3$ and Ag-doped $Bi_2Te_3$ crystals. From the obtained results we discuss the nature of point defects in these crystals.

[1] To whom correspondence should be addressed. E-mail: navratil@pol.upce.cz



0022-4596/98 $25.00

## 2. EXPERIMENTAL

### 2.1. Growth of $Sb_2Te_3$ and $Bi_2Te_3$ Single Crystals with Ag Admixtures

For the preparation of Ag-doped $Sb_2Te_3$ and $Bi_2Te_3$ single crystals 5N-purity Sb, Bi, Te, and Ag were used. Single crystals of $Sb_2Te_3$(Ag) were prepared in two ways:

1. From the melt $Sb_{2-x}Ag_xTe_3$ to incorporate Ag atoms into the Sb sublattice; these crystals are denoted a-$Sb_2Te_3$(Ag).
2. From the melt containing an overstoichiometric content of silver corresponding to the composition $Sb_2Ag_xTe_3$; these crystals are denoted b-$Sb_2Te_3$(Ag).

The single crystals were pulled using the modified Bridgman technique described in refs 16 and 17. The obtained crystals were 50–60 mm long and 10 mm in diameter; they exhibited good cleavability along the (0001) plane. The orientation of the cleavage plane was determined by the Laue back-diffraction technique. The homogeneity of the crystals prepared both ways was checked by comparing the position of the reflectivity minimum $R$ at five points on the surface of the cleaving plane (0001), where the values of $R(v)$ were taken on a circular cut out of diameter 3 mm. The Ag content $c_{Ag}$ in the samples was determined by atomic absorption spectroscopy. The results are shown in Table 1. In a similar way, several single crystals of a-$Bi_2Te_3$(Ag) and b-$Bi_2Te_3$(Ag) with various contents of Ag dopant from the melt were prepared from the melts $Bi_{2-x}Ag_xTe_3$ and $Bi_2Ag_xTe_3$ to compare the properties of Ag-doped $Sb_2Te_3$ and $Bi_2Te_3$. The results of their chemical analysis are given in Table 2. The $c_{Ag}$ values given in Tables 1 and 2 correspond to the number of Ag atoms per $cm^3$.

### 2.2. Measurements of the Electrical Conductivity and the Hall Constant

The Hall constant $R_H(\mathbf{B}\parallel c)$ and the electrical conductivity $\sigma_\perp$ were measured on samples of dimensions $15\times3\times$ (0.1–0.3) $mm^3$ at room temperature. The measurements were realized using alternating current at a frequency of 170 Hz in magnetic field induction $\mathbf{B} = 1.1$ T. The concentration of holes is given by the expression $R_H = r\gamma/pe$, where $r$ is the Hall parameter, $\gamma$ is the structural parameter, $p$ is the hole concentration, and $e$ is the electron charge. The dependence of hole concentration on silver concentration is given in Fig. 1. The value of $r = 1$ and the structural parameter $\gamma = 0.80$ were calculated from data in ref 8.

**TABLE 1**
**Electrical Conductivities and Hall Constants of a-$Sb_{2-x}Ag_xTe_3$ and b-$Sb_2Ag_xTe_3$ Crystals at 300 K**

| Sample | $c_{Ag}$ ($10^{19}$ $cm^{-3}$) | $\sigma_\perp$ ($\Omega^{-1}$ $cm^{-1}$) | $R_H$ ($\mathbf{B}\parallel c$) ($cm^3$ $A^{-1}$ $s^{-1}$) | $\gamma/R_He$ ($10^{19}$ $cm^{-3}$) | $R_H\sigma_\perp$ ($cm^2$ $V^{-1}$ $s^{-1}$) | $\Delta p/c_{Ag}$ |
|---|---|---|---|---|---|---|
| 1a | 0 | 4788 | 0.0590 | 8.43 | 283 | |
| 2a | 2.3 | 5276 | 0.0475 | 10.47 | 251 | 1.57 |
| 3a | 7.0 | 5848 | 0.0284 | 17.52 | 166 | 1.30 |
| 4a | 7.5 | 6195 | 0.0242 | 20.56 | 150 | 1.62 |
| 5a | 8.5 | 7175 | 0.0212 | 23.49 | 152 | 1.77 |
| 1b | 0 | 4788 | 0.0590 | 8.43 | 283 | |
| 2b | 1.5 | 4888 | 0.0443 | 11.23 | 217 | 1.87 |
| 3b | 5.7 | 5720 | 0.0288 | 17.27 | 165 | 1.55 |
| 4b | 8.0 | 6374 | 0.0235 | 21.17 | 150 | 1.59 |
| 5b | 8.2 | 7044 | 0.0195 | 25.51 | 137 | 2.08 |

**TABLE 2**
**Electrical Conductivities and Hall Constants of a-$Bi_{2-x}Ag_xTe_3$ and b-$Bi_2Ag_xTe_3$ Crystals at 300 K**

| Sample | $c_{Ag}$ ($10^{19}$ $cm^{-3}$) | $\sigma_\perp$ ($\Omega^{-1}$ $cm^{-1}$) | $R_H$ ($\mathbf{B}\parallel c$) ($cm^3$ $A^{-1}$ $s^{-1}$) |
|---|---|---|---|
| 1a | 0 | 630 | + 0.41 |
| 2a | 0.71 | 274 | + 0.89 |
| 3a | 0.75 | 207 | + 0.68 |
| 1b | 1.98 | 494 | − 0.49 |
| 2b | 2.34 | 830 | − 0.29 |

### 2.3. Measurements of the IR Reflectivity

Reflectivity spectra in the plasma-resonance frequency range were measured at room temperature in unpolarized light on natural (0001) cleavage faces of the single crystals using a Bio-Rad FTS-45 FT-IR spectrometer. In the measurements the samples were oriented in such a way as to have the electric field vector $\mathbf{E}$ perpendicular to the trigonal axis $c$, i.e., $\mathbf{E}\perp c$. The reflectivity spectra of a-$Sb_2Te_3$(Ag) and b-$Sb_2Te_3$(Ag) are shown in Fig. 2. The reflectivity curves

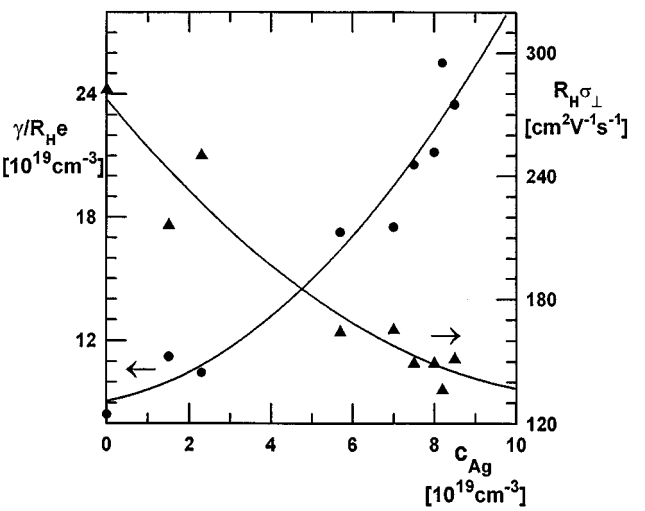


**FIG. 1.** Dependencies of $\gamma/R_He$ and $R_H\sigma_1$ on the Ag content in both a- and b-$Sb_2Te_3$(Ag) single crystals.

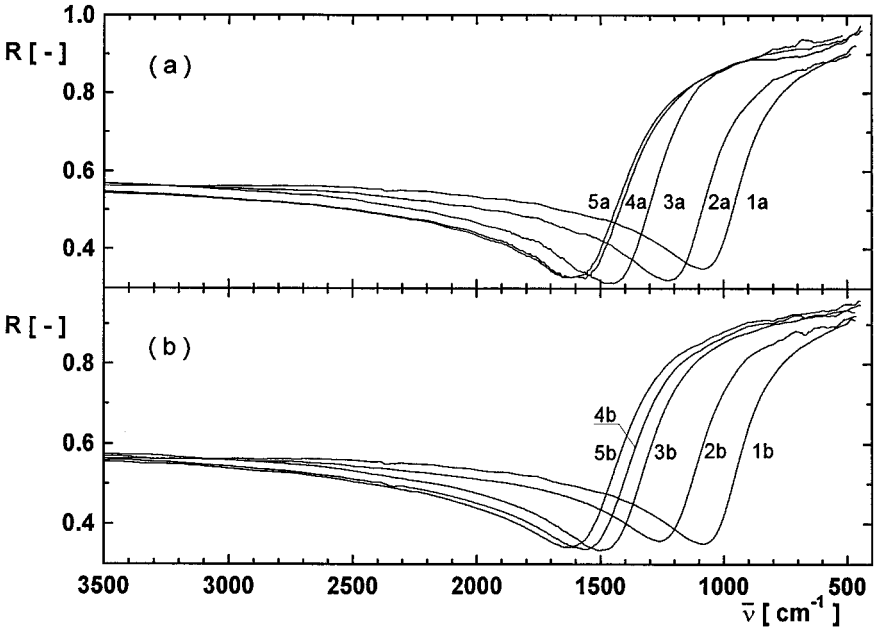


**FIG. 2.** Reflectivity spectra of a- and b-$Sb_2Te_3$(Ag) crystals. The curves are labeled according to Table 1.

$R = f(v)$ clearly show well-defined minima, which confirms that the single crystals are of good quality.

Experimentally obtained dependencies of $R = f(v)$ were evaluated using equations for the real and imaginary parts of the permitivity following the Drude–Zener theory (18).

### *2.4. Determination of Lattice Parameters*

Lattice parameters of the prepared crystals were determined on powder samples by X-ray diffraction analysis using an HZG-4B diffractometer (Freiberger Praezisionsmechanik, Germany). The diffraction maxima were measured by a step procedure using a step size of 0.01°. The measurement was carried out in the range of $2\theta = 5°$–$100°$ with Cu$K\alpha$ radiation; $K\beta$ radiation was removed with a nickel filter. The calibration of the diffractometer was carried out with polycrystalline silicon. The diffraction lines obtained were indexed and the values of the lattice parameters $a$ and $c$ were calculated by the least-squares method.

## 3. RESULTS AND DISCUSSION

From the reflection spectra of $Sb_2Te_3$ doped with various Ag contents, it is evident that the $R = f(v)$ curves manifest a pronounced minimum in the region of plasma resonance frequency. The position of the minimum shifts toward higher wavenumbers with increasing Ag content (Fig. 2). To obtain the changes in the concentration of free current carriers with Ag doping of $Sb_2Te_3$, the experimental $R = f(v)$ curves were modeled using the relations for the real ($\varepsilon_1$) and imaginary ($\varepsilon_2$) parts of the complex dielectric function $\varepsilon$ following the Drude–Zener theory (18):

$$\varepsilon_1 = n^2 - k^2 = \varepsilon_\infty \left(1 - \frac{1}{(\omega/\omega_p)^2 + (1/\omega_p\tau)^2}\right) \quad [1]$$

$$\varepsilon_2 = 2nk = \frac{\varepsilon_\infty}{\omega\tau} \frac{1}{(\omega/\omega_p)^2 + (1/\omega_p\tau)^2}, \quad [2]$$

where $n$ is the index of refraction, $k$ the index of extinction, $\tau$ the optical relaxation time, $\varepsilon_\infty$ the high-frequency dielectric constant, and $\omega_p$ the plasma frequency, which for one kind of free carriers is given by

$$\omega_p = \left(\frac{pe^2}{\varepsilon_0 \varepsilon_\infty m_\perp^*}\right)^{1/2} \quad [3]$$

where $m_\perp^*$ ($= m_\perp m_0$) is the free carrier effective mass in the direction perpendicular to the trigonal axis $c$, $m_0$ is the electron rest mass, $\varepsilon_0$ is the permittivity of free space, and $e$ is the electron charge. Approximate values of $\varepsilon_\infty$, $\tau$, and $\omega_p$ were inserted into Eqs. [1] and [2] and a computer program was used to minimize the function $\sum (R'_n - R_n)^2$, where $R'$ is the experimental reflectance value and $R$ is the value calculated from the relation

$$R = \frac{(n-1)^2 + k^2}{(n+1)^2 + k^2}. \quad [4]$$

Relations [1–4] were used to determine the values of $\varepsilon_\infty$, $\omega_p$, $\tau$, and the ratio $p/m_\perp$ for crystals with various contents of incorporated Ag atoms (see Table 3). The course of the real and imaginary parts of the complex dielectric function for $Sb_{2-x}Ag_xTe_3$ crystals, calculated from the equations of the Drude–Zener theory, is given in Fig. 3, and the spectral dependence of the energy loss function $\mathrm{Im}(-1/\varepsilon)$ is given in Fig. 4. The values of $\varepsilon_2$ increase toward the lower wavenumbers, which is due to the dominant role of free carrier absorption. Maxima of $\mathrm{Im}(-1/\varepsilon)$ for samples 1a–5a correspond with the values $\omega_p$ (see Table 3).

From the frequency dependence of the imaginary part of the dielectric function (see Fig. 3), it is possible to evaluate the type of scattering mechanism of free current carriers. In the frequency region where the scattering is due to free carriers and interband transitions, the imaginary part of the dielectric function is given by the expression

$$\varepsilon_2 = \varepsilon_2^{FC} + \varepsilon_2^{IB}, \qquad [5]$$

where $\varepsilon_2^{FC}$ is the contribution of free current carriers and $\varepsilon_2^{IB}$ is the contribution of interband transitions. According to refs 19 and 20, there is a dependence $\varepsilon_2^{FC} \sim \nu^{-\kappa}$ (where $\kappa$ is the exponent characteristic of the scattering mechanism). This dependence holds for $hvc \gg 2k_BT$.

According to refs 19 and 20, the value of the exponent $\kappa = 2.5$ corresponds to the scattering of free current carriers by acoustic phonons, $\kappa = 3.5$ corresponds to the scattering on the optical branch of lattice vibrations or eventually to piezoelectric scattering, and $\kappa = 4.5$ corresponds to the scattering by ionized impurities. According to our results presented in Fig. 5, the exponent $\kappa$ has the value of $2.9 \pm 0.03$ for all studied a- and b-$Sb_2Te_3$(Ag) crystals. This result does not allow us to make an unambiguous decision on the scattering mechanism of free current carriers, because the validity conditions of the dependence $\varepsilon_2^{FC} \sim \nu^{-\kappa}$ are accomplished only partially. Nevertheless a qualitative conclusion can be done in the following way: the dominant mechanism of free current carriers in the studied crystals is the scattering on acoustical phonons; the observed deviation from the dependence $\varepsilon_2^{FC} \sim \nu^{-2.5}$ indicates the participation of scattering on ionized impurities as well. Such

**TABLE 3**
**Optical Parameters of a- and b-$Sb_2Te_3$(Ag) Crystals**

| Sample | $\varepsilon_{\infty\perp}$ | $\omega_{p\perp}$ Drude–Zener fit ($10^{14}$ s) | $\tau$ ($10^{-14}$ s) | $p/m_\perp$ ($10^{20}$ cm$^{-3}$) |
|---|---|---|---|---|
| 1a | 55.5 | 1.90 | 2.5 | 6.35 |
| 2a | 54.6 | 2.19 | 2.3 | 8.20 |
| 3a | 54.2 | 2.64 | 2.2 | 11.85 |
| 4a | 53.6 | 2.78 | 1.8 | 13.00 |
| 5a | 51.6 | 2.87 | 1.7 | 13.35 |
| 1b | 55.5 | 1.90 | 2.5 | 6.35 |
| 2b | 55.0 | 2.22 | 2.0 | 8.56 |
| 3b | 55.0 | 2.66 | 2.0 | 12.2 |
| 4b | 55.9 | 2.79 | 1.9 | 13.7 |
| 5b | 56.0 | 2.89 | 1.8 | 14.7 |

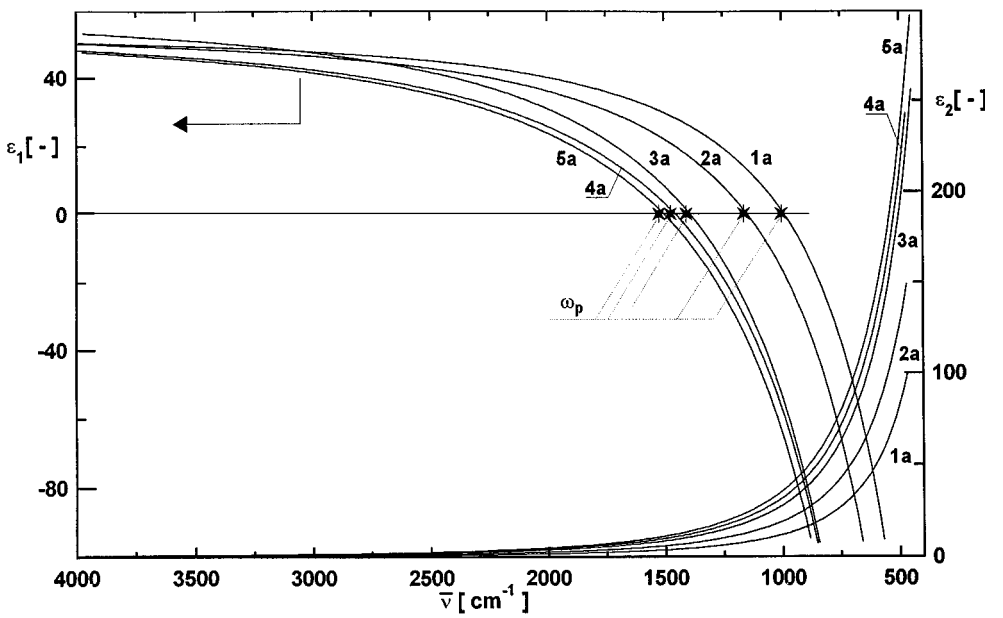


**FIG. 3.** Real ($\varepsilon_1$) and imaginary ($\varepsilon_2$) parts of the permitivity of a-$Sb_2Te_3$(Ag). Locations of plasma resonance frequencies $\omega_p$ obtained from the Drude–Zener theory are indicated. Numbering of dependencies corresponds to Table 3.

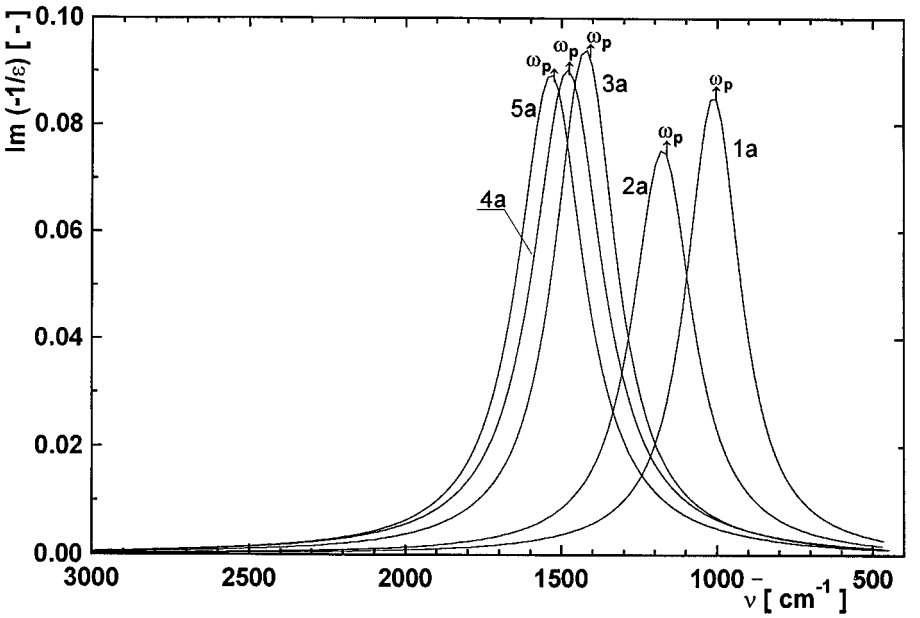


**FIG. 4.** Energy loss function of a-$Sb_2Te_3$(Ag) single crystals obtained from the Drude–Zener relations. Numbering of dependencies corresponds to Table 3.

a qualitative conclusion seems to be correct, as the ferroelectric scattering and the scattering on polar phonons do not seem to take place due to the structure and nature of the chemical bond in the studied crystals. This conclusion is in agreement with the discussion of the relations between the transport coefficients of $Sb_2Te_3$ crystals reported in ref 7.

From Table 3 we can also see that an increase in the content of Ag atoms in $Sb_2Te_3$ results in an increase in the hole concentration in both the crystals obtained from the melt $Sb_{2-x}Ag_xTe_3$ and those obtained from the melt $Sb_2Ag_xTe_3$. The values of the transport parameters (Hall constant, electric conductivity) of the a- and b-$Sb_2Te_3$(Ag)

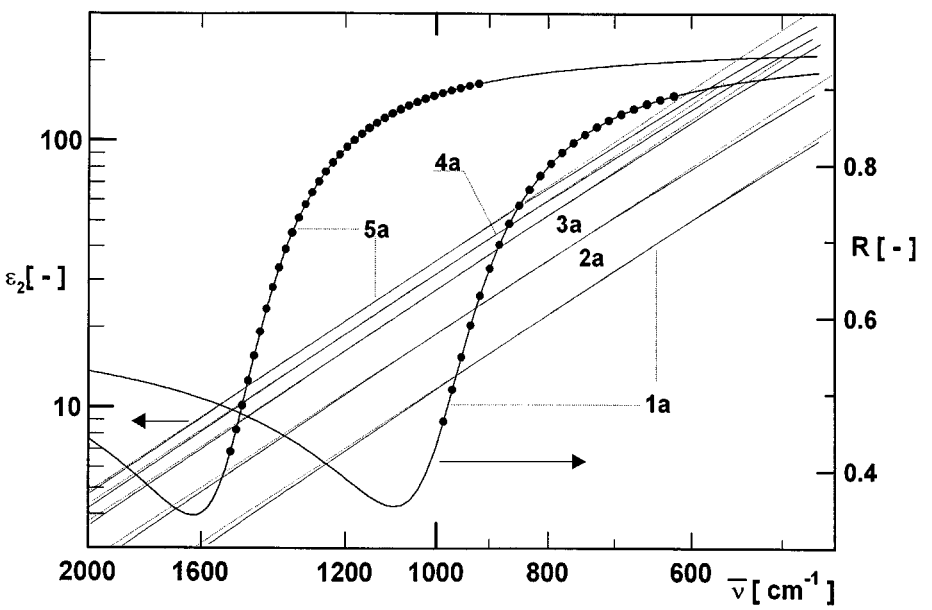


**FIG. 5.** Dependencies $\varepsilon_2$ vs $\nu$ in logarithmic scale. From their slopes, in the wavenumber range where the contribution of the free carriers to $\varepsilon_2$ prevails (range of linear fits is marked by dots on some reflectance curves), values of the $\kappa$ exponent were determined.

crystals with the same concentration of Ag atoms are nearly the same, which is in agreement with the qualitative result of the optical measurements (see Table 2). From the obtained values of $R_H$ an increase in the hole concentration $\Delta p$ caused by the incorporation of Ag atoms was estimated according to the expression

$$[\Delta p] = [\gamma/eR_H(c_{Ag}) - \gamma/eR_H(c_{Ag} = 0)],$$

where $R_H(c_{Ag})$ is the Hall coefficient of $Sb_2Te_3$(Ag) with Ag content $c_{Ag}$ and $R_H(c_{Ag} = 0)$ is the Hall coefficient of the undoped $Sb_2Te_3$ crystal. Using these $\Delta p$ values, we calculated $\Delta p/c_{Ag}$ (see Table 1). The average value of $\Delta p/c_{Ag}$ is 1.7.

The experimental studies gave two results:

1. The studied properties of the a- and b-$Sb_2Te_3$(Ag) crystals with the same value of $x$ are practically the same.

2. Experimental results obtained for crystals grown from the melts $Sb_2Ag_xTe_3$ and $Sb_{2-x}Ag_xTe_3$ show that incorporation of 1 Ag atom into the crystal lattice results in an increase of the free carrier concentration by about 1.7 holes. This finding can be explained by the incorporation of Ag atoms into the cation sublattice. In addition to the $Ag''_{Sb}$ substitutional defects, $[Ag''_{Sb} + h^{\bullet}]$ defects, i.e., $Ag'_{Sb}$, can be formed. We cannot exclude the possible formation of four-layer lamellae of the type $[Ag_{0.5}Sb_{0.5}]$–Te–$[Sb_{0.5}Ag_{0.5}]$–Te, which corresponds to the $AgSbTe_2$ structure, where the crystal planes of the cation sublattice are occupied statistically with Sb and Ag atoms. The formation of four-layer lamellae within the $Sb_2Te_3$ structure does not change any charges and explains the observed decrease in the ratio $\Delta p/c_{Ag}$ from the expected value of 2 to 1.7.

Such results make it possible to qualitatively identify the dominant structural defects in the a- and b-$Sb_2Te_3$(Ag) crystals. The formation of substitutional defects of the type $Ag''_{Sb}$ supports the idea of a possible existence of higher charged defects such as $V'''_{Sb}$ and $V^{\bullet\bullet}_{Te}$. Taking into account this idea, we can describe the incorporation of Ag atoms into the crystal structure by the following equation:

$$2V'''_{Sb} + 3V^{\bullet\bullet}_{Te} + 2Ag(l) + \tfrac{3}{2}Te_2(g) = 2Ag''_{Sb} + 3Te_{Te} + 4h^{\bullet} \quad [6]$$

To incorporate 1 Ag atom into the crystal, resulting in the formation of 2 holes, it is necessary to add to the starting melt not only Ag but also Te in the ratio of 2Ag/3Te. This is fulfilled for the a-$Sb_2Te_3$(Ag) crystals but not for the b-$Sb_2Te_3$(Ag) crystals. A lack of Te in the melt could result in the formation of Te vacancies $V^{\bullet\bullet}_{Te}$ according to Eq. [6] and thus to a change in hole concentration. From the experimental results we have found that a small change in Te concentration in the melt does not change the hole concentration. A possible explanation for this phenomenon can be based on the observation that we obtained crystals with a pronounced overstoichiometric content of Sb from both the $Sb_{2-x}Ag_xTe_3$ and $Sb_2Ag_xTe_3$ melts, as in the case of an undoped $Sb_2Te_3$ crystal grown from the melt of the stoichiometric composition, where segregation of Te takes place and a crystal of composition $Sb_2Te_{2.94-2.97}$ is obtained (21, 22).

The formation of structural defects by Ag atoms in the cation sublattice should be reflected also in changes in the crystal lattice parameters. As the covalent radius of the Ag atom ($r_{Ag} = 0.134$ nm) is smaller than that of the Sb atom ($r_{Sb} = 0.140$ nm), it is possible to expect a smaller elementary cell volume in the crystals containing substitutional defects of $Ag''_{Sb}$. However, the measured lattice parameters of the a- and b-$Sb_2Te_3$(Ag) crystals did not change in comparison to the published data of pure $Sb_2Te_3$ (23). We assume that such a result can be caused by a low content of Ag dopant. Therefore we also prepared samples with a higher Ag content, $Sb_{1.95}Ag_{0.05}Te_3$ and $Sb_{1.9}Ag_{0.1}Te_3$. Their crystal lattice parameters are given in Table 4. It is evident that the elementary cell volume slightly decreases with increasing Ag content. Such a change corresponds to the proposed formation of substitutional defects by Ag atoms replacing Sb atoms in their lattice sites. It is noteworthy that even for crystals with the highest Ag content, i.e., at $Sb_{1.9}Ag_{0.1}Te_3$, we did not observe a diffraction line at $2\theta = 28.799^{\circ}$, which is the strongest line in cubic $AgSbTe_2$.

From the dependence of the Hall constant on the Ag content in $Bi_2Te_3$ crystals given in Table 2, we can see that the increasing concentration of incorporated Ag atoms decreases hole concentrations; at a Ag content of ca. $8 \times 10^{18}$ cm$^{-3}$, the inversion of hole-type conductivity to electron-type conductivity takes place. The simplest explanation for this behavior can be made by considering the formation of positively charged $Ag^{\bullet}_i$ ions situated in interstitial positions of the crystal lattice. Such a result confirms qualitative conclusions published earlier (11).

As presented earlier, the incorporation of Ag atoms into isostructural crystals of $Sb_2Te_3$ and $Bi_2Te_3$ results in the formation of different point defects in these crystals. The formation of different point defects can be associated with the differences in their lattice parameters but also with the

**TABLE 4**
**Lattice Parameters of $Sb_{2-x}Ag_xTe_3$ Crystals**

| Composition $x$ | $a$ (Å) | $c$ (Å) | $V$ (Å$^3$) |
|---|---|---|---|
| 0 | 4.2648(3) | 30.450(1) | 479.6(1) |
| 0.05 | 4.2623(7) | 30.446(4) | 479.0(2) |
| 0.10 | 4.2619(5) | 30.443(4) | 478.9(1) |

different chemical bonding (in spite of that in a first approximation it seems to be very similar). To outline the differences in the chemical bonding, we present here some results of the calculation of bonding parameters obtained by the quantum chemical program MOPAC 93. Input data, definitions of bonding parameters, and the calculation procedure are given in the Appendix. In Table 5 the values of charges on the individual atoms and bond order are given for both isostructural tellurides. As these parameters are closely linked to the interatomic distances in the tetradymite structure, we add in Table 5 also the interatomic distances obtained by the total crystallographic analysis. Such a semiempirical calculation gives qualitative data on the chemical bonding in the studied tellurides.

As can be seen from the obtained data, the bond order $BO^1$ of the Sb–$Te^1$ bonds and $BO^2$ of the Sb–$Te^2$ bonds are significantly higher than the bond order $BO^1$ of the Bi–$Te^1$ bonds and $BO^2$ of the Bi–$Te^2$ bonds, respectively. The bonds between Bi and Te atoms in the $Bi_2Te_3$ crystal have a higher ionicity than the bonds between Sb and Te in the $Sb_2Te_3$ crystal. This result is also consistent with the values of charges on the individual atoms of the crystal lattice. The negative charge on the $Te^1$ and $Te^2$ atoms in the $Bi_2Te_3$ crystal is approximately one order higher than the negative charge on the same atoms in the $Sb_2Te_3$ crystal. Also the Bi atoms in the $Bi_2Te_3$ crystal have a higher positive charge by one order than the Sb atoms in the $Sb_2Te_3$ crystal.

The calculated charges of the atoms in the cation and anion sublattices of both tellurides $Me_2Te_3$ (where *Me* is Sb or Bi) comply with the bonding model given in ref 24. The model considers $6s^2$ electrons of $Te^2$ atoms as bonding which together with the $6p^4$ electron of $Te^2$ and the five electrons of the Bi atoms with the contribution of one electron of the $Te^1$ atom form $sp^3d^2$ hybrid orbitals which form stronger bonds than the individual Bi–$Te^1$ bond. In agreement with this model the calculated value of the charge on the $Te^2$ atoms is considerably higher than that on the $Te^1$ atoms in both compounds. A small charge on the $Te^1$ atoms and a higher value of $BO^1$ than $BO^2$ manifest a substantial covalent character of the $Te^1$–*Me* chemical bond, whereas the $Te^2$–*Me* bond has a higher contribution of an ionic character. Due to the lower charge on the $Te^1$ atoms of the $Sb_2Te_3$ crystal, we could assume smaller repulsion forces between $Te^1$ layers adjacent to the van der Waals gap and thus a smaller width of the van der Waals gap in comparison to $Bi_2Te_3$; the parameters of the van der Waals gap given in ref 25 agree well with this conclusion, unlike those given in ref 26.

**TABLE 5**
**Charge on Individual Atoms and Structural Parameters of $Sb_2Te_3$ and $Bi_2Te_3$**

| | $Sb_2Te_3$ | $Bi_2Te_3$ |
|---|---|---|
| Interatomic distance | | |
| *Me*–$Te^1$ | 2.98 | 3.07 |
| *Me*–$Te^2$ | 3.17 | 3.25 |
| $Te^1$–$Te^1$ | 3.74 | 3.64 |
| Atomic charge | | |
| $Te^1$ | − 0.044 | − 0.57 |
| *Me* | 0.087 | 1.04 |
| $Te^2$ | − 0.085 | − 0.94 |
| Bond order | | |
| $BO^1$(*Me*–$Te^1$) | 0.538 | 0.522 |
| $BO^2$(*Me*–$Te^2$) | 0.240 | 0.154 |

We assume that such extraordinary large differences in the bonding parameters of both tellurides determine also the behavior of these crystals on incorporation of foreign atoms into their crystal lattice and also their mutual solubility in the solid state. By mutual solubility we mean in this case the ability of Ag atoms to enter positions in the cation sublattice, i.e., the formation of mixed crystals. The different forms of incorporation of Ag atoms into the $Sb_2Te_3$ and $Bi_2Te_3$ crystal structures (in the $Sb_2Te_3$ structure, Ag atoms replace Sb atoms; in the $Bi_2Te_3$ structure, Ag forms interstitial defects) can be derived also from the different structures of $AgSbTe_2$ and $AgBiTe_2$ (12). The low-temperature modification of $AgBiTe_2$ forms a pseudohexagonal structure belonging to the space group $D^3_{3d}$ (according to ref 12, $a = 0.437$ nm, $c = 2.076$ nm, and the unit cell consists of three layers formed by four Ag–Te–Bi–Te atomic planes). This modification is unstable at 300 K and atmospheric pressure. The similar compound $AgSbTe_2$ is stabilized by the transformation to the pseudocubic NaCl structure (12), derived from the trigonal, pseudohexagonal structure $D^3_{3d}$-$P3m1$.

This transformation can be realized in such a way that the cation sublattice formed in the pseudohexagonal structure $AgSbTe_2$ by the planes of Ag and Sb atoms is occupied statistically by Ag and Sb atoms. In this way, a more stable structure is formed, characterized by alternating planes of Te–$(Sb_{0.5}Ag_{0.5})$–Te–$(Ag_{0.5}Sb_{0.5})$ with the same mutual interplanar distances. In such a way, the $D^3_{3d}$ structure transforms into a more stable cubic structure (the trigonal *c* axis is coincident with the diagonal of the cubic cell).

From the foregoing description of the structure of the $AgSbTe_2$ crystal, it is evident that the Ag atoms can form substitutional defects in layered tellurides with a similar structure. These data can be taken as a support for our model of the incorporation of Ag atoms into $Sb_2Te_3$ crystals in the form of $Ag''_{Sb}$ substitutional defects.

## 4. CONCLUSIONS

Some dopants of the I group of the periodic table incorporated into tetradymite-type crystals can behave as both donors and acceptors. For example, Cu atoms incorporated

into $Bi_2Se_3$ crystals (27) behave as acceptors when added to the $Bi_2Se_3$ melt in the ratio 2Cu/3Se, but when added to the $Bi_2Se_3$ melt as an overstoichiometric surplus, they behave as donors. We observed the same effect in Cu-doped $Bi_2Te_3$ crystals.

We have shown that Ag atoms in $Sb_2Te_3$ crystals always behave as acceptors, regardless of whether Ag dopant is added as an overstoichiometric surplus or in stoichiometric proportion compensated by Te addition in the ratio of 2Ag/3Te. We assume the reason for this effect can probably be found in the overstoichiometric Sb content in the crystals grown from the melt of both compositions, which gives rise to a relatively high concentration of $Sb'_{Te}$ antisite defects. Therefore the shortage of Te in the $Sb_2Ag_xTe_3$ melt has no influence on the hole concentration.

We have concluded from the experiments that in $Sb_2Te_3$(Ag) crystals $Ag''_{Sb}$ substitutional defects are formed. This conclusion makes it possible to assume an existence of defects with higher charges such as $V'''_{Sb}$ and $V^{\bullet\bullet}_{Te}$, as described in Eq. [6]. This idea seems to be supported by the fact that in the crystal structure of the isostructural $Bi_2Te_3$ crystal the existence of $V'''_{Bi}$ and $V^{\bullet\bullet}_{Te}$ defects has been proven on the basis of theoretical considerations in ref 28.

Whereas Ag atoms in the $Sb_2Te_3$ structure form $Ag''_{Sb}$ defects, in $Bi_2Te_3$ crystals Ag atoms are probably incorporated as $Ag^{\bullet}_i$ interstitials. Thus doping Ag atoms form different types of defects in $Sb_2Te_3$ and $Bi_2Te_3$. The differences in the incorporation of doping Ag atoms into the $Sb_2Te_3$ and $Bi_2Te_3$ crystal structures are probably due to the significant differences in the parameters of chemical bonding. The ability of Ag atoms to form $Ag_{Sb}$ substitutional defects can be explained by the close values of the covalent radii of the Ag and Sb atoms.

In $Sb_2Te_3$(Ag) crystals the mechanism of scattering of free carriers on acoustical phonons prevails. The expected contribution of the scattering on ionized impurities, which does not change with crystal composition, is not surprising. This finding is also supported by the results obtained in ref 7.

## 5. APPENDIX

To compare the nature of chemical bonding in the isostructural crystals $Sb_2Te_3$ and $Bi_2Te_3$ using the bonding parameters, we used the quantum-chemical program MOPAC 93 (Modified Neglect of Diatomic Overlap (PM3)) to calculate the charges on individual atoms of the investigated crystal lattice.

Since the studied crystals exhibit a relatively narrow energy gap and a considerable concentration of the free charge carriers, we respected the requirement given in the manual (29), namely that the crystal section used to calculate the chemical bond parameters should have sufficiently large dimensions and suitable shape. Therefore, the calculations were carried out for a section of a crystal layer between the van der Waals gap, which contained 120 atoms and had a prismatic shape, approximately 20 Å in the $x$–$y$ plane. At the same time, we fulfilled the required conditions to close the chosen spatial form in such a way that conserved bonds between the initial and final atomic plane.

### *Definition of the Notions Used*

Electron density refers to one atom and is given in units of elementary charge. It is given by the main diagonal members of the density matrix (29). Atomic charge is calculated on the basis of the determined electron density, with respect to the number of electrons on an atom. Bond order between $A$ and $B$ atoms is an average order of the bonds of the same kind. It describes the multiplicity of a bond (i.e., corresponds to the electron density in the space occupied by a bond), is a dimensionless quantity denoted by BO, and is given by the equation

$$\mathrm{BO}_{AB} = \sum_{\lambda \in A} \sum_{\sigma \in B} P^2_{\lambda\sigma} \qquad [7]$$

where $P^2_{\lambda\sigma}$ is an element of the density matrix.

## ACKNOWLEDGMENT

This work was supported by Grant HTECH CRG 960850 NATO.

## REFERENCES

1. R. Sehr and L. R. Testardi, *J. Phys. Chem. Solids* **23,** 1219 (1962).
2. M. Stordeur, *in* "CRC Handbook of Thermoelectrics" (D. M. Rowe, Ed.), p. 239. CRC Press Inc., Boca Raton, New York, London, Tokyo, 1995.
3. A. von Middendorf, K. Dietrich, and G. Landswehr, *Solid State Commun.* **13,** 443 (1973).
4. H. Köhler and A. Freudenberger, *Phys. Status Solidi B* **84,** 195 (1977).
5. G. Simon and N. Eichler, *Phys. Status Solidi B* **107,** 201 (1981).
6. V. A. Kulbachinskii, Z. M. Dashevskii, M. Inoue, M. Sasaki, H. Negishi, W. X. Gao, P. Lošťák, J. Horák, and A. de Viser, *Phys. Rev. B* **52,** 10915 (1995).
7. M. Stordeur, *Phys. Status Solidi B* **98,** 199 (1980).
8. M. Stordeur, H. T. Langhammer, H. Sobotta, and V. Riede, *Phys. Status Solidi B* **104,** 513 (1981).
9. M. Stordeur and G. Simon, *Phys. Status Solidi B* **124,** 799 (1984).
10. J. Horák, P. Lošťák, L. Šiška, and M. Stordeur, *Phys. Status Solidi B* **114,** 39 (1982).
11. B. M. Goltsman, V. A. Kudinov, and I. A. Smirnov, *in* "Poluprovodnikovyje Thermoelektricheskie Materialy na Osnove $Bi_2Te_3$," p. 58. Izdatel'stvo Nauka, Moscow, 1972.
12. S. Geller and J. H. Wernick, *Acta Crystallogr.* **12,** 46 (1959).
13. A. Stegherr, F. Wald, and P. Eckerhin, *Z. Naturforsch. A* **16,** 130 (1961).
14. R. A. Burmeister and D. A. Stevenson, *Trans. Metallurg. Soc. AIME* **230,** 329 (1964).
15. R. A. Burmeister and D. A. Stevenson, *J. Appl. Phys.* **34,** 1833 (1963).

16. P. Lošťák, R. Novotný, L. Beneš, and S. Civiš, *J. Cryst. Growth* **94,** 656 (1989).
17. J. Navrátil, P. Lošťák, and J. Horák, *Cryst. Res. Technol.* **26,** 675 (1991).
18. T. S. Moos, G. J. Burrell, and B. Ellis, *in* "Semiconductor opto-electronics," p. 36. Butterworth & Co., Ltd., 1973.
19. M. Stölzer, M. Stordeur, H. Sobotta, and V. Riede, *Phys. Status Solidi B* **138,** 259 (1986).
20. K. Seger, *in* "Semiconductor Physics," pp. 160, 343. Springer-Verlag, Berlin, Heidelberg, New York, 1982.
21. G. Offergeld and J. van Cakenberghe, *J. Phys. Chem. Solids* **11,** 310 (1959).
22. J. Horák, Č. Drašar, R. Novotný, S. Karamazov, and P. Lošťák, *Phys. Status Solidi A* **149,** 549 (1995).
23. F. Hulliger, *in* "Structural Chemistry of Layer Type Phases" (F. Lévy, Ed.), p. 197. Riedel, Dordrecht, Boston, 1976.
24. J. R. Drabble and C. H. L. Goodman, *J. Phys. Chem. Solids* **5,** 142 (1958).
25. N. Kh. Abrikosov *et al*., "Semiconducting II–VI, IV–VI, and V–VI Compounds." Plenum Press, New York, 1969.
26. F. Hulliger, *in* "Structural Chemistry of Layer Type Phases" (F. Lévy, Ed.), p. 198. Riedel, Dordrecht, Boston, 1976.
27. A. Vaško, L. Tichý, J. Horák, and J. Weissenstein, *Appl. Phys.* **5,** 217 (1974).
28. P. Pecheur and G. Toussaint, *J. Phys. Chem. Solids* **55,** 327 (1994).
29. J. J. P. Stewart, "MOPAC 93.00 Manual." Fujitsu Ltd., Tokyo, Japan, 1993.